Available online at www.sciencedirect.com
ScienceDirect
Journal of Solid State Chemistry 180 (2007) 1103–1109
JOURNAL OF SOLID STATE CHEMISTRY
www.elsevier.com/locate/jssc

Electronic structure, galvanomagnetic and magnetic properties of the bismuth subhalides Bi_4I_4 and Bi_4Br_4

T.G. Filatova[a], P.V. Gurin[b], L. Kloo[c], V.A. Kulbachinskii[b], A.N. Kuznetsov[a,*], V.G. Kytin[b], M. Lindsjo[c], B.A. Popovkin[a]

[a]*Department of Chemistry, Moscow State University, 119992 Leninskie Gory 1-3, GSP-2, Moscow, Russian Federation*
[b]*Department of Physics, Moscow State University, 119992 Leninskie Gory 1-2, GSP-2, Moscow, Russian Federation*
[c]*Department of Chemistry, Royal Institute of Technology, S-100 44 Stockholm, Sweden*

Received 23 October 2006; received in revised form 27 December 2006; accepted 5 January 2007
Available online 20 January 2007

Abstract

Two bismuth-rich subhalides, Bi_4Br_4 and Bi_4I_4, featuring extended quasi one-dimensional metallic fragments in their structures, have been investigated. The gas-phase technique of crystal growth has been refined for obtaining large (up to 5 mm long) single crystals. Electronic structure calculations on three-dimensional structures of both compounds have been performed (DFT level, hybrid B3LYP functional), predicting a semiconducting behavior for both compounds, with an indication of possible directional anisotropy of electric conductivity. Galvanomagnetic (resistance, magnetoresistance, Hall effect, thermopower) and magnetic (temperature and field dependence of magnetization) properties have been measured experimentally. Both compounds are found to be diamagnetic, room-temperature semiconductors with n-type conductivity. While Bi_4Br_4 demonstrates a typical case of one dimensionality, the difference in magnetoresistivity between Bi_4Br_4 and Bi_4I_4 indicates some weak interactions between isolated bismuth metallic fragments within the bismuth substructures.

Keywords: Bismuth-rich compounds; Subhalides; Low-dimensional structures; Electronic structure; Conductivity; Magnetic properties

1. Introduction

A small number of different bismuth subhalides have been reported in literature. Their crystal structures feature either bismuth cluster polycations Bi_9^{5+}: $BiCl_{1.167}$ [1,2], Bi_7Cl_{19} [3], and $BiBr_{1.167}$ [4], or extended one-dimensional polymer molecules formed by corrugated bismuth stripes or ribbons of varying width, terminated from two sides by halogen atoms. Such four atom-wide ribbons were found in the structures of Bi_4Br_4 [4], Bi_4I_4 [5–7], Bi_4BrI_3, $Bi_4Br_2I_2$, and Bi_4Br_3I [8], and 14 and 18 atom-wide ribbons were found in $Bi_{14}I_4$ [9] and $Bi_{18}I_4$ [10], respectively. The geometry of bismuth–bismuth bonds within a single polymer molecule in such subhalides and the two-dimensional corrugated layer present in the structure of bismuth metal is almost identical.

One-dimensional polymer molecules in the compounds in question are stacked into two-dimensional fragments that, in turn, are parallel to each other and comprise a three-dimensional molecular crystal lattice. Since, as is evident from the respective interatomic distances [11], molecules and stacks are rather weakly bonded to each other, the crystals are expected to be highly anisotropic. While the crystal structures of such compounds have been extensively studied over the years, data on their electrical and magnetic properties are very scarce.

According to Ref. [6], bismuth monoiodide crystallizes in three different modifications; two of them, α- and β-Bi_4I_4, have been structurally characterized and differ only slightly in the way of stacking of the polymeric entities. The structure of bismuth monobromide [4] is highly related to the both monoiodide modifications. All three phases crystallize in the monoclinic space group $C2/m$. The fragment of Bi_4Br_4 structure is shown in Fig. 1.

*Corresponding author. Fax: +7 495 9390998.
E-mail address: alexei@inorg.chem.msu.ru (A.N. Kuznetsov).

0022-4596/$ - see front matter © 2007 Published by Elsevier Inc.
doi:10.1016/j.jssc.2007.01.010

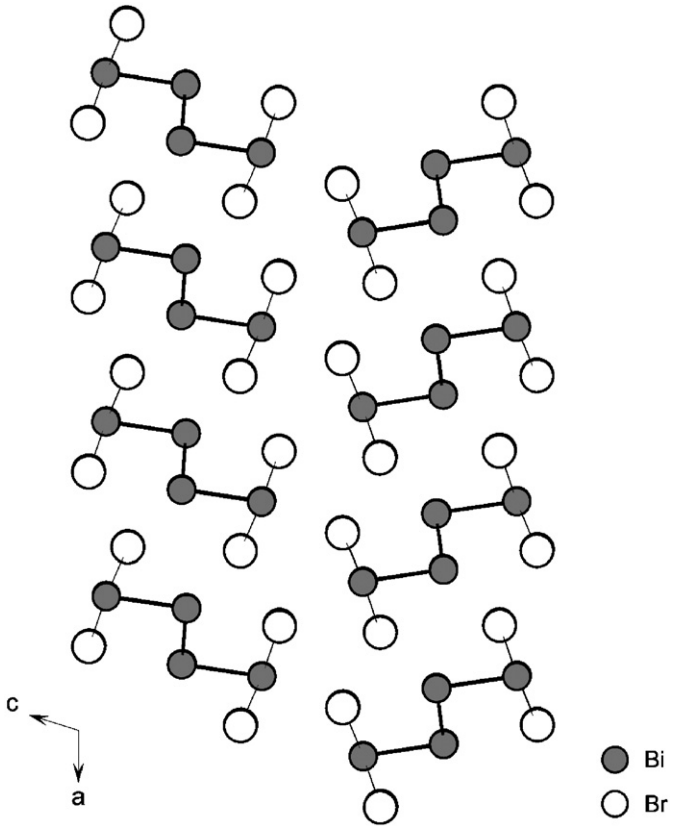

Fig. 1. A fragment of Bi_4Br_4 structure, showing the spatial arrangement of the Bi_4Br_4 strips.

Resistivity measurements in the temperature range 4–300 K along the longer axis of Bi_4Br_4 crystals [4], performed on two samples, displayed a minimum at about 80 K and maximum at about 200 K. The authors of Ref. [4] were unable to determine the absolute value of resistivity due to difficulties in properly measuring the cross-section of the crystals. No further literature data on the electrical conductivity of other compounds of this type appear to exist. The reports concerning magnetic properties essentially only propose a diamagnetic behavior of Bi_4I_4 (molar magnetic susceptibility at room temperature is -111×10^{-6} cm^3/mol [5]). No computational data are available on electronic structures of such compounds.

The present work combines results from a computational study of the electronic structures of Bi_4Br_4 and Bi_4I_4 with extensive experimental studies of the electrical and magnetic properties of single crystals and powders of these two compounds.

2. Experimental

2.1. Synthesis

Single crystals of Bi_4Br_4 and Bi_4I_4, respectively, were obtained from gas phase reactions according to the methods similar to that described in Refs. [4,6]. Thoroughly ground mixtures of bismuth metal and HgI_2 or Hg_2Br_2 were used as starting materials. Bismuth to mercury halide molar ratios in different experiments were either 4:1 or 2:1, with a total amount of approximately 2 g. Silica ampoules with the length of 20–25 cm and inner diameter of 10 or 15 mm were used for crystal growth. The duration of the experiments varied from 24 to 72 h. Ampoules were dried under dynamic vacuum (ca. 0.01 Torr) prior to their use, then one end was filled with the reaction mixture, and the ampoules were flame-sealed under vacuum and placed into a slightly tilted horizontal two-temperature furnace in such a way that the hotter end containing the mixture was in a lower position than the empty colder one. Two combinations of cold/hot end temperatures were used: 165/275 and 200/278 °C.

Single crystals of Bi_4I_4 were obtained as black needles or as elongated flexible platelets. The shape of the crystals was primarily dependent of the inner diameter of the ampoules used. Bundles of multiple needle-like crystals up to 1 mm long were obtained on the walls of the ampoules with 15 mm inner diameter at 200–250 °C temperatures. When using ampoules with a smaller inner diameter (10 mm), we observed the formation of platelets and needles up to 5 mm long in the temperature zone around and over the mixture. According to X-ray powder diffraction (XRPD) data ($CuK_{\alpha 1}$ radiation, Guinier camera FR-552, Enraf-Nonius), both types of crystals were β-Bi_4I_4 [6], and according to EDX data (CAMEBAX SX-50) atomic percentages of bismuth and iodine, averaged over 3 points, were 49.4 and 49.7, respectively, which are within the margin of error (ca. 1 at%) to the Bi_4I_4 formula. XRPD data also indicated that bismuth metal and $Bi_{14}I_4$ were always present in the bulk after the reaction. In all cases a pinkish substance was visible in the cold end of the ampoules. This compound was identified as Hg_2I_2.

Single crystals of Bi_4Br_4 were obtained as black needles up to 2 mm in length or very thin flexible platelets up to 3 mm in length and 0.5 mm in width on the walls of the ampoules in the 210–230 °C temperature zone. The composition of the crystals was confirmed by XRPD and EDX analyses (average bismuth and bromine content was 49.1 and 50.4 at%, respectively). According to XRPD data, the rest of the bulk contained bismuth metal, as well as visible droplets of mercury. It should be noted that our attempts to follow the authors of Ref. [4] and obtain Bi_4Br_4 crystals from the mixture of Bi and $HgBr_2$ (3:1 molar ratio and total amount of approximately 2 g; heating the reaction ampoules for 3 days in the temperature gradient 200/270 °C) were unsuccessful. A microcrystalline substance was observed to have formed in the 200–250 °C zone; using XRPD analysis it was identified as $BiBr_3$.

Powdered samples of the compounds were synthesized by annealing of stoichiometric mixtures of Bi and I in the case of Bi_4I_4, and of Bi and $BiBr_3$ (produced by the direct reaction between bismuth metal and gaseous bromine at 250–260 °C) in the case of Bi_4Br_4. The duration of annealing was 30 days at 260 °C for Bi_4Br_4, and 60 days

at 300 °C for β-Bi_4I_4. The composition and purity of the samples were confirmed by XRPD.

2.2. Electronic structure calculations

Quantum chemical calculations on the three-dimensional structures of Bi_4Br_4 [4] and α-Bi_4I_4 [6] were performed using the hybrid density functional B3LYP employing the CRYSTAL98 program package [12]. The effective large-core potentials (ECPs) by Hay and Wadt (HAYWLC) were utilized for bismuth, bromine and iodine, and original unchanged Hay and Wadt valence basis sets were used to represent bromine and iodine valence shells [13]. The original Hay and Wadt bismuth valence basis set was expanded and optimized for better performance (see Table 1). Convergence on energy was achieved in each case.

2.3. Physical measurements

2.3.1. Galvanomagnetic properties

The resistance was measured with the four-probe method in the temperature interval 4–280 K. To single crystals of typical size $2 \times 0.05 \times 0.01$ mm (Bi_4Br_4) and $1 \times 0.2 \times 0.01$ mm (Bi_4I_4) 4 contacts were soldered. Magnetoresistance and the Hall effect at different temperatures were also determined. Measurements were made in the direction of elongation of a needle-like single crystal. Magnetoresistance and the Hall effect at different temperatures in magnetic fields up to 6 T provided by a superconducting solenoid was recorded. Measurements of thermopower were performed at room temperature on pressed powdered samples, synthesized by the ampoule method described above.

2.3.2. Magnetic properties

Magnetic properties of single crystals of Bi_4I_4 and Bi_4Br_4 were investigated using a SQUID magnetometer. The temperature dependence of magnetization, $M(T)$ in a low external magnetic field (H) of 200 Oe was determined. For the zero field cooled (ZFC) measurements the samples were cooled from room temperature down to 5 K in the absence of magnetic field. They were subsequently heated in a magnetic field of 200 Oe and the magnetization was recorded as a function of temperature. For field cooled (FC) measurements, the samples were cooled from 310 to 5 K in a field of 200 Oe and subsequently heated in the same field. The magnetization was measured as a function of temperature.

The field dependence of the magnetization, $M(H)$ was also studied. The samples were subjected to a magnetic field cycling between +10 and −10 kOe, and the magnetization was measured as a function of magnetic field at temperatures of 5 and 300 K.

Table 1
Optimized valence basis set for bismuth (for use with the original HAYWLC ECP)

Shell	Exponent
s	0.6240
s	0.3550
s	0.1350
p	1.1550
p	0.3300
p	0.1451
d	0.1200

3. Results and discussion

3.1. Band structure and bonding

From the wavefunctions of Bi_4Br_4 and Bi_4I_4, as calculated from their known three-dimensional periodic structures, projected and total densities of states of these two compounds were obtained, as illustrated in Figs. 2 and 3, respectively. Based on the data obtained, both compounds should exhibit semiconducting behavior (the estimated corresponding band gaps are 0.6 and 0.8 eV). Calculated atomic charges: for Bi_4Br_4—Bi (inner) +0.17, Bi (terminal) +0.40, Br −0.31; for Bi_4I_4–Bi (inner) +0.16, Bi (terminal) +0.19, I −0.18. It is clear that due to the higher electronegativity of bromine, as compared to iodine, terminal bismuth atoms (i.e. those connected to halogen atoms) bonded to bromine carry significantly higher positive charge than the corresponding terminal bismuth

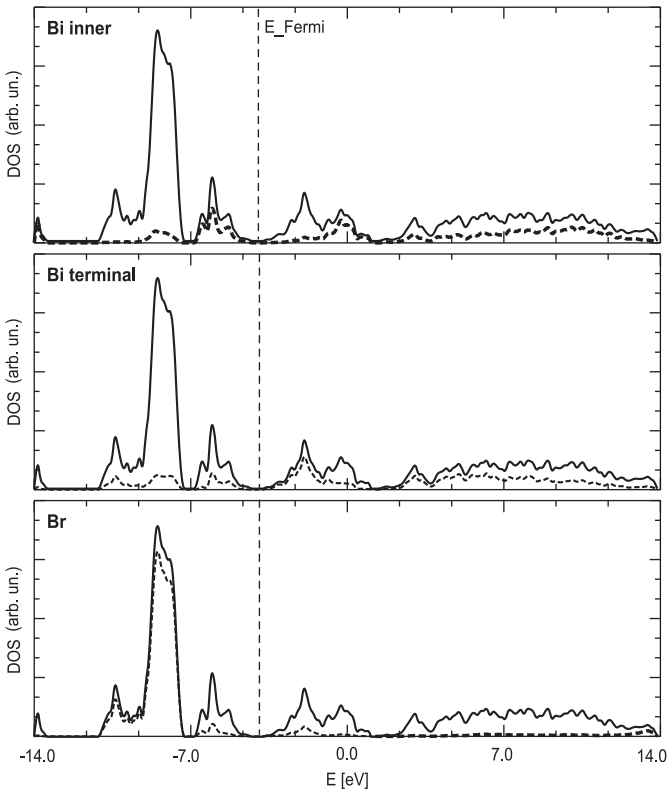

Fig. 2. Calculated projected (dashed line) and total (solid line) DOS for Bi_4Br_4 structure.

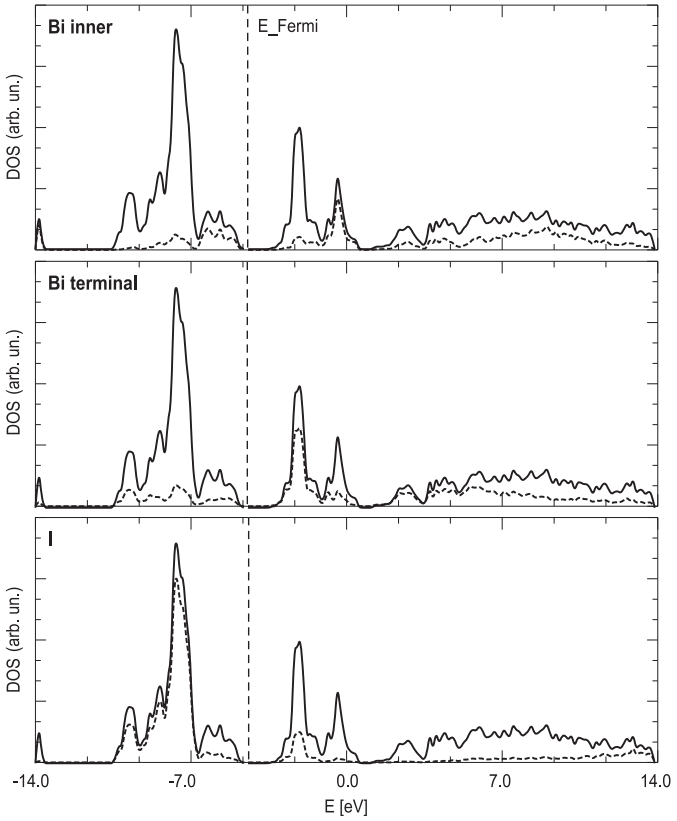

Fig. 3. Calculated projected (dashed line) and total (solid line) DOS for Bi_4I_4 structure.

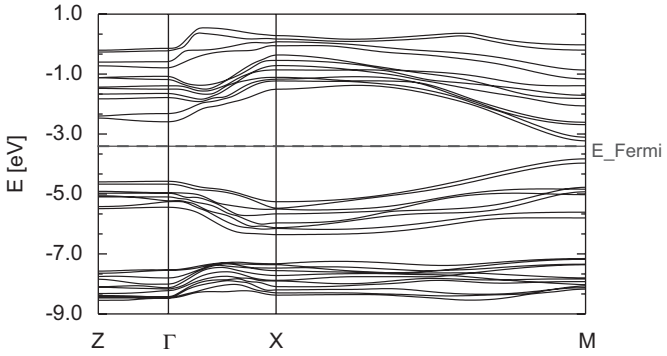

Fig. 4. Band structure of Bi_4Br_4.

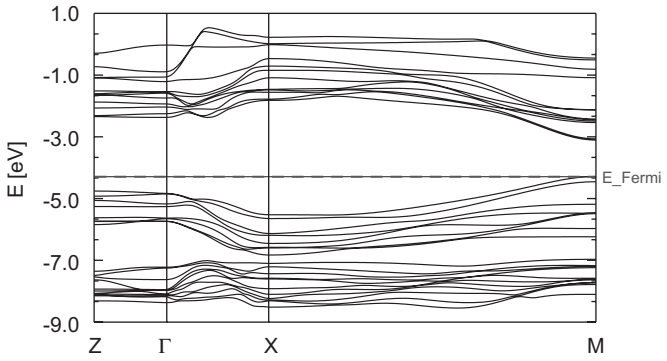

Fig. 5. Band structure of Bi_4I_4.

atoms bonded to iodine atoms, while the charge differences between inner bismuth atoms in both structures are rather small. Figs. 2 and 3 also demonstrate that halogen *p*-states in both phases are almost filled and contribute largely to the valence bands of the respective compounds. Bismuth atoms provide a significant contribution to the conduction bands, with the states of inner and terminal bismuth atoms residing almost in the same energy range. Evidently, *p*-states of both types of bismuth atoms contribute to a certain degree to the bonding to halogen atoms, while *s*-states (6*s* lone pairs) are far below the Fermi level and do not provide any contribution to the bonding. The only significant difference between inner and terminal bismuth atoms, visible in the density of states (DOS), is at the bottom of the valence bands, with the energy lower than about -8.2 eV. In this region of the DOS only the contributions from terminal bismuth atoms and halogens are significant.

Band structures near the Fermi level for Bi_4Br_4 and Bi_4I_4 are given in Figs. 4 and 5, respectively. Qualitatively they are similar and confirm the general semiconducting behavior of these subhalides derived from DOS calculations. It may be noted that along the *X*–*M* direction the bands come rather close to the Fermi level as compared to other spatial directions. This direction corresponds to the *ab* plane of the unit cell, i.e. the propagation of bismuth strips. Thus, these pictures might be taken as an indication of anisotropic behavior; however, since at no point Fermi level directly crosses bands in any compound, this suggested anisotropy is of quantitative rather than qualitative nature and does not change the semiconducting behavior of both subhalides.

3.2. Magnetic properties

ZFC and FC temperature dependences of the magetization [$M(T)$] for Bi_4Br_4 are shown in Fig. 6. Very similar dependences were obtained for Bi_4I_4, but the absolute value is approximately 3 times lower. Magnetization as a function of magnetic field [$M(H)$] is shown in Fig. 7 for a single crystal sample of Bi_4I_4, after subtracting the diamagnetic contribution from the sample holder. Similar data were obtained for Bi_4Br_4. As observed from the figures, both materials show diamagnetic behavior. The very small deviation from ideal diamagnetic behavior observed at $B = 0$ in Fig. 7 may be caused by a small amount of some ferromagnetic impurity present in starting materials or introduced during crystal growth from the components. Since this ferromagnetism is very weak, it can most probably be ascribed to the presence of magnetic impurities with high Curie temperatures (such as iron or nickel). EDX analyses were performed on the samples, but no impurities could be identified down to the limit of detection of the technique. The decrease of magnetization seen in the ZFC $M(T)$ data at low temperatures indicates spin freezing.

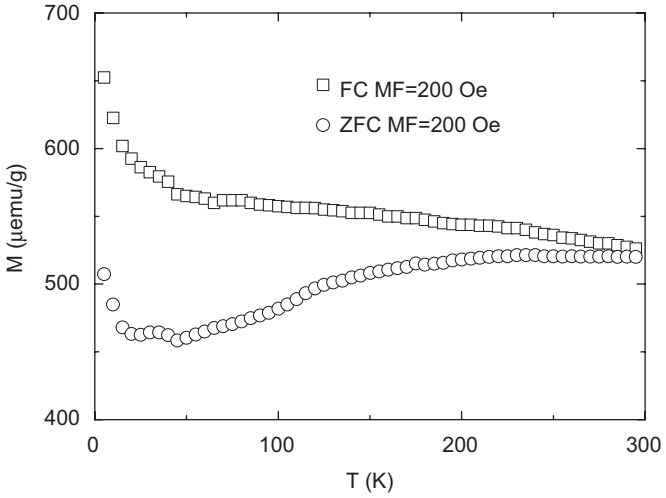

Fig. 6. $M(T)$ data for a single crystal of Bi_4Br_4.

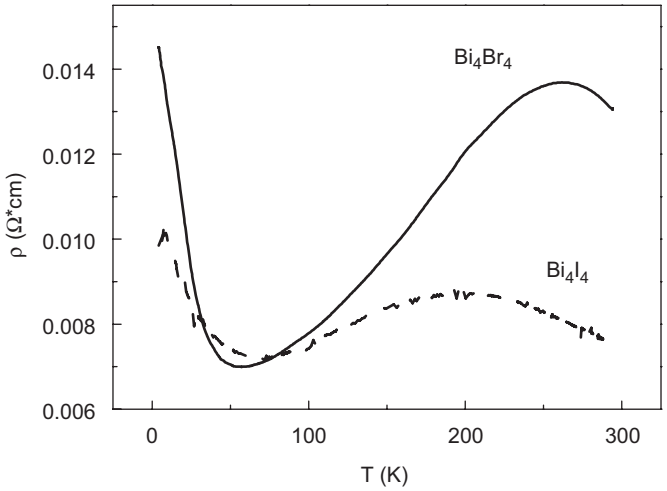

Fig. 8. Temperature dependence of resistance.

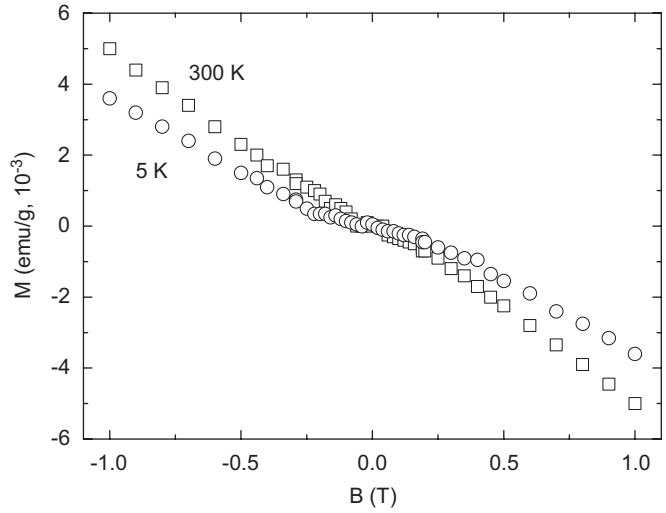

Fig. 7. $M(H)$ data at 300 K and 5 K after subtracting the diamagnetic contribution from the sample holder for a single crystal of Bi_4I_4.

We would also like to highlight a peculiarity in the $M(T)$ dependence at $T = (55–60\,K)$. In this temperature range the temperature dependence of resistance changes from metallic-like (typical for both metals and degenerate semiconductors) to that of a non-degenerate semiconductor (see below). At $T < 20\,K$ magnetization increases and clearly shows the presence of paramagnetic impurities discussed above.

3.3. Galvanomagnetic properties

The temperature dependences of the resistivity ρ for the two samples are shown in Fig. 8. Two similar features can be clearly seen in the temperature dependence of resistivity for both Bi_4Br_4 and Bi_4I_4. A maximum of resistivity is observed at $T \approx 260\,K$ for B_4Br_4 and at $T \approx 220\,K$ for Bi_4I_4. Close to $T = 55\,K$ the character of $\rho(T)$ changes from metallic-like to that of a non-degenerate semiconductor. At the same time, the absolute values of resistivity confirm that both compounds remain semiconductors over the whole temperature range, so the resistivity minimum must correspond to the transition between non-degenerate and degenerate semiconductor behavior. We must note here, that the resistivity minimum for Bi_4Br_4 was observed by the authors of Ref. [4] and attributed to the transition between extrinsic and intrinsic conductivity. However, our Hall effect measurements (see below) do not agree with such interpretation, since they show no significant change in carrier concentration both above and below the temperature of the resistivity minimum. (In addition, the authors of [4] did not have the absolute resistivity values and, therefore, could not distinguish on that basis between a metal and degenerate semiconductor.)

We believe that such dielectrization of the energy spectrum may be ascribed to a charge density wave (CDW) transition. For a direct proof of the CDW at low temperature additional experiments would be required. The dependence of the drop in electric potential recorded for the samples upon application of an external magnetic field consists of even and odd parts with respect to the magnetic field. According to convention we related the odd part to the magnetoresistance, $R(B)$. In both systems this function displays positive values. The magnetoresistance of Bi_4I_4 at different temperatures is shown in Fig. 9a. At low magnetic fields B, $R(B)$ shows a quadratic dependence on B at all temperatures studied. At $T = 21\,K$ for $B > 2\,T$, $R(B)$ follows a linear relation with respect to the external magnetic field. The magnetoresistance of Bi_4Br_4 is shown in Fig. 9b. At $T = 4.2$ and 23 K $R(B)$ saturates and at $T = 76\,K$ it is very weak and displays a quadratic behavior.

Traditionally, the even part of the dependence of a drop in electric potential upon application of an external magnetic field to a sample is explained by the Hall effect. The irregular geometry of the samples suggests that only a fraction of the true Hall resistance can be calculated from the even part of the drop in electric potential. Further, we

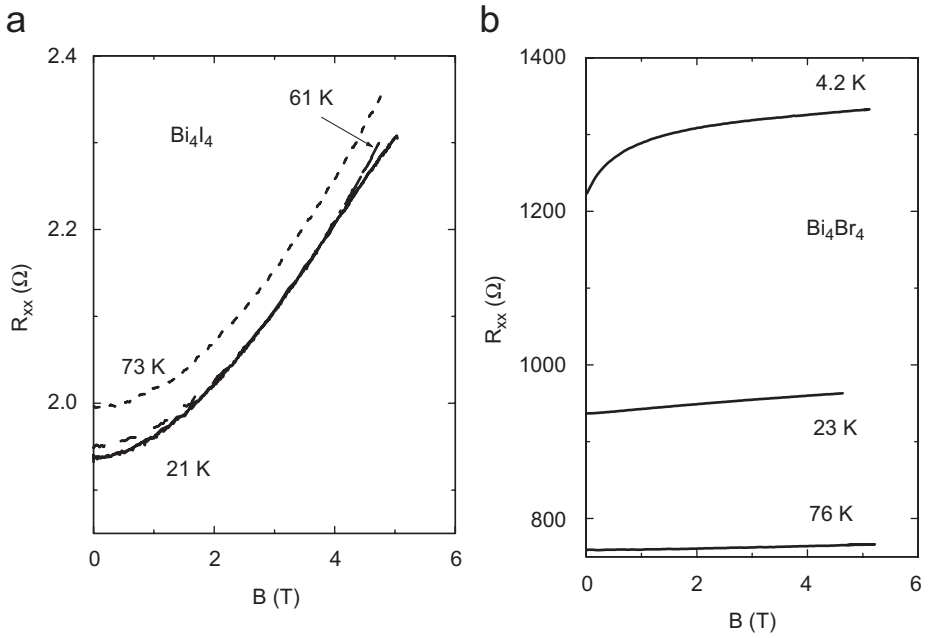

Fig. 9. Magnetoresistance of Bi_4I_4 (a) and Bi_4Br_4 (b).

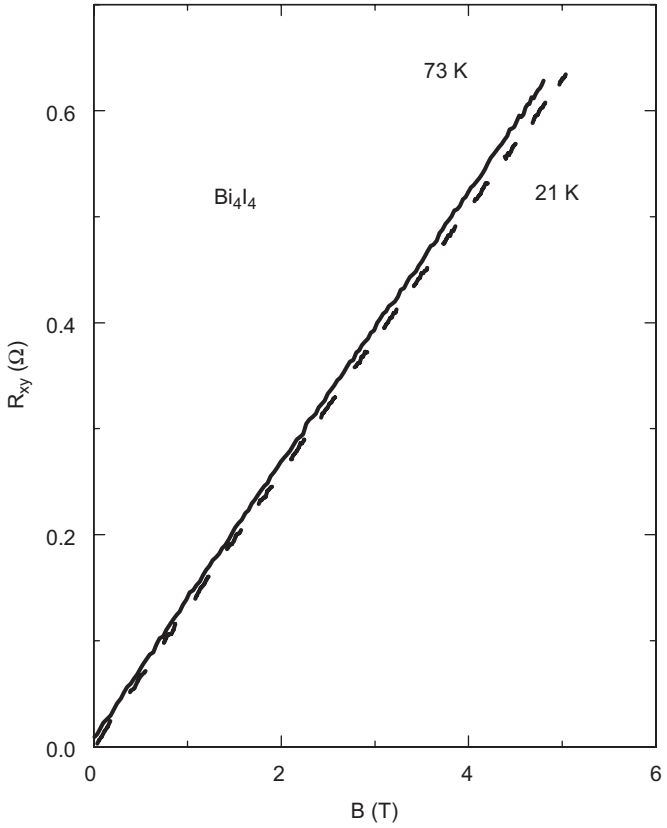

Fig. 10. Dependence of the Hall resistance on the external magnetic field for Bi_4I_4 at two different temperatures.

denote this fraction as R_{xy}. As an example, the dependence of R_{xy} on B is shown in Fig. 10 for Bi_4I_4 at two different temperatures.

As seen in Fig. 10, $R_{xy}(B)$ follows a linear function with respect to B. From these data it is strongly suggested that there is only one type of charge carriers in Bi_4I_4. The magnetic field dependence of $R_{xy}(B)$ in Bi_4Br_4 is similar. The irregular geometry of the samples, and in particular the irregular cross-section of the samples, makes it impossible to extract the carrier concentration from the Hall effect. The measurements of thermopower performed on pressed powder samples showed that the Seebeck coefficient is negative for both Bi_4Br_4 and Bi_4I_4 (at 300 K the values are -82 and $-200\,\mu V/K$, respectively). Thus, the charge carriers are electrons in both samples. Those data indicate that the position of the Fermi level, which is determined by carrier concentration (which in turn is determined by defects of the crystal structure, in addition to the intrinsic properties of electronic structure), differs from that shown in Figs. 2 and 3, the band structures of the ideal crystals at zero temperature. The maxima of temperature dependence of resistivity observed at high temperatures can then be explained by thermal activation of electrons to the conduction band. The presence of two close conduction bands may be seen in the band structures (see Figs. 4 and 5). Thus, we suggest that the minima of resistivity observed at temperatures close to 50 K are caused by the formation of a CDW in the quasi-one-dimensional degenerate semiconductors Bi_4Br_4 and Bi_4I_4 [14]. The observed positive magnetoresistance in Bi_4Br_4 (see Fig. 9b) is typical for quasi-one-dimensional semiconductors and metals [14,15]. In Bi_4I_4 (see Fig. 9a) the magnetoresistance is different and somewhat more similar to that of three-dimensional materials. One reason for this is the less ionic character of bonding in this material, as

compared to Bi_4Br_4 (see below), and the more three-dimensional character of the energy spectrum.

4. Conclusions

In conclusion, we would like to emphasize several points derived from the analysis of the combined theoretical and experimental data. First of all, all the results from the theoretical calculations of electronic structures of bismuth subbromide and subiodide and the predicted respective properties are in good agreement with the experimental results. As is evident from both computational and experimental data, both compounds predominantly exhibit semiconducting behavior. Moreover, it has been shown that electrons are the charge carriers in both cases (n-type conductivity). This correlates very well with the fact that bismuth metal is an n-type conductor and a poor metal (or semi-metal) in terms of electric conductivity. Both subhalide structures only contain fragments of very limited width, which essentially correspond to the two-dimensional layers of bismuth atoms in pure metal, where a certain degree of electron delocalization must be present. These fragments, terminated by electronegative halogen atoms, evidently do not have the same charge carrier concentration as bismuth metal, thus resulting in a semiconducting behavior. The change from degenerate to non-degenerate semiconductor at very low temperatures might involve phase transitions; however, helium-temperature X-ray crystallography is required in order to clarify the exact nature of the structural changes, indicating a change in bonding pattern, causing the alterations in the conducting behavior.

A comparison of the behavior of the two subhalides highlights a general similarity in their electronic structures as well as physical properties, with one notable exception. Of particular interest is the difference in the magnetoresistance of Bi_4Br_4 and Bi_4I_4 (see Fig. 9). As mentioned above, bismuth monobromide shows a classic one-dimensional behavior, which is to be expected because of the pronounced quasi-one-dimensional structural fragments in the compound. Strangely enough, Bi_4I_4, which is formally iso-structural with Bi_4Br_4, demonstrates serious deviations from one dimensionality. However, this can be rationalized using both our theoretical and experimental data. As seen from the calculations, relative charges on bismuth atoms are lower in the case of Bi_4I_4 (because of the higher electronegativity of Br, as compared to I), making it a better n-conductor, also confirmed by the experimental resistivity measurements (see Fig. 8). Therefore, more electrons take part in delocalization, making it possible for neighboring bismuth strips to interact with each other. These interactions, while no doubt too weak to be considered bonding, could still in our view somewhat "contaminate" pure one dimensionality of bismuth subiodide in contrast to one-dimensional subbromide.

Acknowledgments

Prof. Dr. K.V. Rao and Dr. L. Belova from Stockholm Royal Institute of Technology are gratefully acknowledged for the magnetic measurements. This work was supported by RFBR (grant Nos. 05-03-08186-ofi and 06-03-32789) and Russian Presidential Grants Council (grant No. MK-688.2006.3).

References

[1] A. Hershaft, J.D. Corbett, J. Chem. Phys. 36 (1962) 551–552.
[2] J. Beck, C.J. Brendel, L. Bengtsson-Kloo, B. Krebs, H. Mummert, A. Stankovsky, S. Ulvenlund, Chem. Ber. 129 (1996) 1219–1226.
[3] S. Hampel, P. Schmidt, M. Ruck, Z. Anorg. Allg. Chem. 631 (2005) 272–283.
[4] H. von Benda, A. Simon, W. Bauhofer, Z. Anorg. Allg. Chem. 438 (1978) 53–67.
[5] B. Predel, D. Rothacker, Termochim. Acta 2 (1970) 477–487.
[6] H.G. von Schnering, H. von Benda, C. Kalveram, Z. Anorg. Allg. Chem. 438 (1978) 37–52.
[7] E. Dikarev, B. Popovkin, Moscow Univ. Bull. 31 (1990) 496–499.
[8] E.V. Dikarev, B.A. Popovkin, A.V. Shevelkov, Russ. Chem. Bull. Int. Ed. 50 (2001) 2304–2309.
[9] E.V. Dikarev, B.A. Popovkin, A.V. Shevelkov, Z. Anorg. Allg. Chem. 612 (1992) 118–122.
[10] E.V. Dikarev, B.A. Popovkin, Dokl. Chem. 310 (1990) 117–120.
[11] E.V. Dikarev, A.V. Shevelkov, B.A. Popovkin, Mendeleev Chem. J. 36 (1991) 276–287.
[12] V.R. Saunders, R. Dovesi, C. Roetti, M. Causa, N.M. Harrison, R. Orlando, C.M. Zicovich-Wilson, CRYSTAL98, University of Turin, Turin, 1998.
[13] P.J. Hay, W.R. Wadt, J. Chem. Phys. 82 (1985) 284–298.
[14] Y. Takahide, S. Uji, K. Enomoto, T. Konoike, T. Terashima, M. Nishimura, T. Tsuneta, K. Inagaki, S. Tanda, K. Yamaya, Phys. Rev. B. 71 (2005) 134409.
[15] J. Heremans, C.M. Thrush, Z. Zhang, X. Sun, M.S. Dresselhaus, J.Y. Ying, D.T. Morelli, Phys. Rev. B. 58 (1998) R10091.